

# X-Ray Diffraction Evidence for the Extensibility of Actin and Myosin Filaments during Muscle Contraction

Katsuzo Wakabayashi,\* Yasunobu Sugimoto,\* Hidehiro Tanaka,† Yutaka Ueno,\* Yasunori Takezawa,\* and Yoshiyuki Amemiya§

\*Department of Biophysical Engineering, Faculty of Engineering Science, Osaka University, Toyonaka, Osaka 560, Japan; †Department of Physiology, Teikyo Heisei College of Nursing, Ichihara, Chiba 290-01, Japan; and §Photon Factory, National Laboratory for High Energy Physics, Tsukuba, Ibaraki 305, Japan

**ABSTRACT** To clarify the extensibility of thin actin and thick myosin filaments in muscle, we examined the spacings of actin and myosin filament-based reflections in x-ray diffraction patterns at high resolution during isometric contraction of frog skeletal muscles and steady lengthening of the active muscles using synchrotron radiation as an intense x-ray source and a storage phosphor plate as a high sensitivity, high resolution area detector. Spacing of the actin meridional reflection at  $\sim 1/2.7 \text{ nm}^{-1}$ , which corresponds to the axial rise per actin subunit in the thin filament, increased about 0.25% during isometric contraction of muscles at full overlap length of thick and thin filaments. The changes in muscles stretched to  $\sim$ half overlap of the filaments, when they were scaled linearly up to the full isometric tension, gave an increase of  $\sim 0.3\%$ . Conversely, the spacing decreased by  $\sim 0.1\%$  upon activation of muscles at nonoverlap length. Slow stretching of a contracting muscle increased tension and increased this spacing over the isometric contraction value. Scaled up to a 100% tension increase, this corresponds to a  $\sim 0.26\%$  additional change, consistent with that of the initial isometric contraction. Taken together, the extensibility of the actin filament amounts to 3–4 nm of elongation when a muscle switches from relaxation to maximum isometric contraction. Axial spacings of the layer-line reflections at  $\sim 1/5.1 \text{ nm}^{-1}$  and  $\sim 1/5.9 \text{ nm}^{-1}$  corresponding to the pitches of the right- and left-handed genetic helices of the actin filament, showed similar changes to that of the meridional reflection during isometric contraction of muscles at full overlap. The spacing changes of these reflections, which also depend on the mechanical load on the muscle, indicate that elongation is accompanied by slight changes of the actin helical structure possibly because of the axial force exerted by the actomyosin cross-bridges. Additional small spacing changes of the myosin meridional reflections during length changes applied to contracting muscles represented an increase of  $\sim 0.26\%$  (scaled up to a 100% tension increase) in the myosin periodicity, suggesting that such spacing changes correspond to a tension-related extension of the myosin filaments. Elongation of the myosin filament backbone amounts to  $\sim 2.1 \text{ nm}$  per half sarcomere. The results indicate that a large part ( $\sim 70\%$ ) of the sarcomere compliance of an active muscle is caused by the extensibility of the actin and myosin filaments; 42% of the compliance resides in the actin filaments, and 27% of it is in the myosin filaments.

## INTRODUCTION

In muscle contraction, the force of the acto-myosin motor is transmitted to the ends of the contractile unit through thin actin filaments, which have generally been thought to contribute very low compliance to the mechano-chemical machinery. The evidence for low compliance in actin filaments originally came from stiffness measurements of sarcomeres during activation of intact muscles at various lengths. The stiffness of the muscle was dependent on the amount of overlap between the thick and thin filaments in the manner expected if thin filament extensibility accounts for less than  $\sim 20\%$  of the total sarcomere compliance of a fiber resulting from the combination of cross-bridge compliance in series with thin filament compliance (Huxley and Simmons, 1973; Ford et al., 1977, 1981). The remainder of the mechanical compliance was then considered to reside in the actomyosin cross-bridges between the two sets of filaments. In that case, the stiffness (the reciprocal of compliance) would be a useful

signal related to the number of cross-bridges attached to the actin filaments (Ford et al., 1977, 1981). However, the assumption that the myofilaments are effectively inextensible under active tension cannot be verified.

On the one hand, extensibility of the thin filament has been suggested by flexural rigidity measurements of actin filaments (e.g., Oosawa, 1977) and by electron microscopic studies on the stretch-induced lengthening of the sarcomere in rigor fibers (Suzuki and Sugi, 1983). Stiffness measurements of active muscle fibers at full overlap have indicated that a certain proportion of sarcomere compliance is localized in the actin filament (Julian and Morgan, 1981; Bagni et al., 1990). Most recently, the stiffness of the actin-tropomyosin complex was directly measured by in vitro nano-manipulation, indicating that the actin filaments are purely elastic and extensible (Kojima et al., 1994). Precise measurement of the sarcomere stiffness in rigor at short lengths showed a much larger contribution of the thin filaments to the sarcomere compliance than previous mechanical studies (Higuchi, Yanagida, and Goldman, unpublished data).

It is well known that in x-ray diffraction patterns, the reflections arising from the thick myosin filaments indicate an axial spacing increase by about 1–1.4% when live vertebrate muscle contracts isometrically at full filament overlap

Received for publication 12 April 1994 and in final form 7 July 1994.

Address reprint requests to Dr. Katsuzo Wakabayashi, Department of Biophysical Engineering, Osaka University, Toyonaka, Osaka 560, Japan. Tel.: 06-850-6515; Fax: 06 843 9354; E-mail: waka@bpe.es.osaka-u.ac.jp.

© 1994 by the Biophysical Society

0006-3495/94/12/2422/14 \$2.00

(Huxley and Brown, 1967; Haselgrove, 1975; Bordas et al., 1993; also see below). This spacing change itself is too large to be attributable to a direct effect of isometric tension on the thick filament compliance (Ford et al., 1981). The spacing change occurs ahead of the tension change during the onset of a contraction and recovers much more slowly than the tension decline during relaxation (Huxley et al., 1982; Faruqi, 1986). Several recent experiments have dissociated this spacing change from actual force production (Huxley et al., 1982, 1988; Yagi et al., 1993; Bordas et al., 1993). For instance, the spacing does not return to the resting value when the muscle is shortening near its maximal velocity and tension is virtually zero (Yagi et al., 1993). The spacing increase also takes place when the muscle is put into rigor with or without development of tension (Haselgrove, 1975; Yagi, 1992). Thus, the increase in spacing of reflections related to the myosin periodicity on contraction is not caused only by tension. Much of the large change has been attributed to the formation of cross-bridge attachments to the thin filaments accompanying a large change in the helical order of the cross-bridges (Huxley et al., 1982, 1988; Bordas et al., 1993). However, the full nature of the spacing change in the myosin periodicity is still unclear and some of the change may also be caused by extensibility of the filaments themselves.

The constancy of the axial spacing of the actin filament-based 5.9 nm reflection (within  $\sim 0.5\%$ ) during isometric contraction in earlier x-ray diffraction experiments (Huxley and Brown, 1967; Haselgrove, 1975) has often been quoted as evidence for inextensibility of the thin filaments. However, x-ray diffraction evidence on this point has hitherto been unreliable because of technical limitations. In the present work to clarify the mechanics of actin and myosin filaments in muscle, we carefully examined spacing changes of reflections in the x-ray diffraction patterns caused by the thin and thick filament structures. Using intense synchrotron x-rays from a storage ring at the Photon Factory (Tsukuba, Japan) and a high sensitivity, high resolution integrating area detector, small spacing changes of the reflections arising from the actin and myosin filaments during isometric contraction and steady lengthening of the active muscle could be recorded with improved accuracy.

Changes in the axial spacing of actin reflections were investigated at full-,  $\sim$ half-, and nonoverlap (estimated by isometric force) between the thin and thick filaments in the sarcomere. We show that the extensibility of the actin filaments under maximum isometric tension is small but significant. This extensibility is associated with a slight change of the helical symmetry. The effects of steady lengthening applied to contracting muscles on the actin and myosin filament-based reflections are described, showing extensibility of the myosin filaments too. Finally, contribution of the extensibility of both filaments to the instantaneous sarcomere elasticity is discussed. A preliminary account of this work has been reported in abstract form (Wakabayashi et al., 1992, 1993).

## MATERIALS AND METHODS

### Specimens and contraction experiments

Sartorius and semitendinosus muscles of the bullfrog (*Rana catesbeiana*) were used for this study. They were mounted in a specimen chamber with a multi-electrode assembly. The pelvic end of the muscle was clamped to the chamber while the tibial end or tendon was connected to a force transducer. The sarcomere length was adjusted to three different values at  $\sim 2.3$ ,  $3\text{--}3.2$ , and  $>4\text{ }\mu\text{m}$  by optical diffraction of He-Ne laser light. For the sarcomere lengths of  $4\text{--}4.4\text{ }\mu\text{m}$ , the semitendinosus muscle was used; a dorsal branch of the muscle was slowly stretched to the nonoverlap length and then left at long length at least 30 min before experiments to minimize the effect of passive tension (Huxley, 1973; Kress et al., 1986). The filament overlap was finally determined by measuring the isometric force (see below). The chamber was continuously perfused with chilled ( $10^\circ\text{C}$ ) and oxygenated Ringer's solution (115 mM NaCl, 2.5 mM KCl, 1.8 mM  $\text{CaCl}_2$ , pH adjusted to 7.2 with  $\text{NaHCO}_3$ ). The muscle was stimulated isometrically for 1.3 s with trains of 3 ms supramaximal current pulses at 33 Hz. The maximum isometric force was  $2.0\text{--}2.8\text{ kg/cm}^2$  at  $\sim 2.3\text{ }\mu\text{m}$ , about half that at  $3\text{--}3.2\text{ }\mu\text{m}$  and less than  $0.2\text{ kg/cm}^2$  at  $>4\text{ }\mu\text{m}$  sarcomere length. The three lengths by their isometric force are designated as sarcomere lengths for full-, half-, and nonoverlap of the thin and thick filaments. The passive tension of over-stretched muscles decayed over  $\leq 30$  min to a comparable level with or less than the maximum isometric tension at this same sarcomere length. Each muscle was tetanized 10–15 times at resting intervals of 30 s until force declined to a level of about 85% of the initial value. The average tensions at full- and half-overlap were in the range of  $2.0\text{--}2.6\text{ kg/cm}^2$  and  $1.0\text{--}1.3\text{ kg/cm}^2$ , respectively, and the tension remained nearly unchanged at nonoverlap.

Slow stretch experiments were made; a muscle at full overlap length was first kept isometric, and when the isometric tension reached its plateau, constant-velocity stretches ( $3\text{--}4\%$  of the initial muscle length ( $L_0$ )/s) were applied using a moving-coil driver controlled with a feed-back circuit. The muscles were stimulated with trains of 3 ms current pulses for 3 s at  $8^\circ\text{C}$ . The force at the end of stretch was  $50\text{--}70\%$  above the isometric contraction level. Slow stretch applied during contraction was repeated 10–11 times for each muscle at intervals of 1 min. The experiments were terminated when the isometric tension of muscles declined to less than 80% of that in the initial stimulation.

### X-ray diffraction techniques

The experiments were done at Beam Line 15A of the Photon Factory (Tsukuba, Japan) using a small-angle diffractometer (Amemiya et al., 1983; Wakabayashi and Amemiya, 1991). Synchrotron x rays (wavelength,  $0.151\text{ nm}$ ) from a positron storage ring, operated at  $2.5\text{--}3\text{ GeV}$  with a ring current between 250 and 300 mA were selected and collimated with double focusing optics. The focused beam size was  $0.8\text{ mm}$  (vertical)  $\times$   $0.7\text{ mm}$  (horizontal). Two-dimensional x-ray diffraction patterns from the muscles set vertically were recorded on a storage phosphor area detector (an imaging plate) (e.g., Amemiya et al., 1987, 1988) with a spatial resolution of  $100\text{ }\mu\text{m}$ . Using the same muscles, the patterns in the resting state and at the plateau phase of isometric tension in muscles at full- and half-overlap or upon stimulation of overstretched muscle were recorded separately on the imaging plates for 1.0 s. Total exposure for each condition was 10–15 s.

The x-ray beam was directed onto the specimen at right angles to the fiber axis. The specimen axis was not tilted to optimize the meridional reflection at  $\sim 1/2.7\text{ nm}^{-1}$ , because the tilt angle needed to center this reflection on the sphere of reflection is so small ( $\sim 1.6^\circ$  at the  $0.151\text{ nm}$  wavelength) that the curvature of the sphere of reflection can be assumed to be practically flat. Because the reflections are "arced" by  $3\text{--}4^\circ$  because of the natural dispersion of filament orientation within the muscles, the effect of the tilt would be insignificant providing that the profile of the reflection is not significantly altered during contraction (see below). The specimen-to-detector distance was set at  $\sim 150\text{ cm}$  to record reflection lines up to  $\sim 1/2\text{ nm}^{-1}$  reciprocal spacing on the  $18\times 18\text{ cm}^2$  imaging plate.

For the experiments in which slow stretches were applied to contracting muscles, a device to rapidly exchange  $12.6\times 12.6\text{ cm}^2$  imaging plates was

employed in combination with a fast shutter system (Amemiya et al., 1989; Amemiya and Wakabayashi, 1991). Diffraction patterns were recorded for 0.8 s during the isometric plateau and during the stretch. Total exposure time for each condition was 8–8.8 s. A shorter camera length was used ( $\sim 100$  cm). Because of the smaller size of the detector used in this system, the actin reflection at  $\sim 1/2.7 \text{ nm}^{-1}$  could not be recorded simultaneously with other low-angle reflections.

In both types of experiment, care was taken that the pelvic end of the muscle was fixed firmly to hooks in the chamber after applying a few short tetanic stimuli to the muscle to ensure that the specimen axis did not move during stimulation. In this way, the diffraction patterns during repetitive stimulations could be summed on the same imaging plates.

### Data treatment and spacing measurements

The data on the imaging plates were read at  $100 \mu\text{m}$  pixel spacing using the drum-scanner described by Amemiya et al. (1988) and stored on magnetic tape. The different plates were read at the same orientation to minimize scanning errors of the image reader. The digitized data were converted into the format of the image processing system (by Y. Ueno) on a NEC ACOS S-3700 computer (the Protein Institute of Osaka University). They were analyzed on high resolution graphic workstations (PC-98RL, NEC and Spark Station 330, Sun Microsystems) to precisely determine parameters such as the position of the direct beam and the inclination angle of the meridian in the image. Among many diffraction patterns, high quality paired patterns with filament angular dispersion of  $3\text{--}4^\circ$  relative to the fiber axis (as determined by the angular deconvolution method (Makowski, 1978)) were selected and used for the analysis. After determining the origin and correcting the inclination angle accurately, the four quadrants of the patterns were averaged and data from two or three muscles were summed to attain greater signal-to-noise ratios. The intensities between the resting and activated patterns from all muscles were normalized by the total intensity in the whole area of the diffraction pattern (except for the strongest parts on the equator) or by the intensities in the same selected area near the corner of images where reflections were not present.

Spacing changes were analyzed for three relatively strong actin filament-based reflections; the meridional reflection at  $\sim 1/2.7 \text{ nm}^{-1}$  and the two layer-line reflections at  $\sim 1/5.1 \text{ nm}^{-1}$  and  $\sim 1/5.9 \text{ nm}^{-1}$ . Hereafter, the three reflections are identified using the real spacings unless otherwise stated. Spacing measurements of the meridional reflection were made in the reciprocal radial range of  $0 \leq R \leq 0.053 \text{ nm}^{-1}$  ( $R$  denotes the radial coordinate in reciprocal space), parallel to the equator to cover a main peak profile. The spacings of the 5.1 and 5.9 nm layer-line reflections were initially measured in the same radial range (the inner part of the whole layer line), where the layer lines appeared straight because of the minimal effect of disorientation of filaments within the muscle (see Holmes and Barrington-Leigh, 1974). However, there are meridional peaks of nonhelical origin at axial spacing very near both of these two actin layer lines, so we finally settled on measuring the spacings in the radial range of  $0.013 \leq R \leq 0.053 \text{ nm}^{-1}$  to exclude the meridional peaks (see below). The spacings of the myosin filament based-meridional reflections such as the third (M3), sixth (M6), ninth (M9), and fifteenth (M15) orders of the basic 42.9 nm repeat were measured in the radial range of  $0 \leq R \leq 0.032 \text{ nm}^{-1}$ , where most of their intensity was located. The intensities in the above ranges were first summed by radial integration, and then intensity distributions across the several layer lines were obtained in the axial direction. Because the three actin reflections partially overlapped neighboring myosin reflections (see below), the raw data points were fitted using several overlapping Gaussian peaks by an in-house program based on a nonlinear least-squares method (a modified Marquardt method; e.g., see Press et al. (1990) written for the Sun View system by Y. Sugimoto). The background intensity was fitted and stripped out by either a polynomial function or an appropriate Gaussian function with its peak at the origin. This Gaussian deconvolution technique enabled us to determine the centroid of the reflection profiles to an accuracy better than 0.05%. In the slow stretch experiments, only the spacings of the 5.1, 5.9, M3, M6, and M9 reflections were measured. Spacing changes reported in this article are expressed as a percentage of the resting spacing except for the slow stretch experiments in which they are shown as a percentage of the initial isometric contraction value.

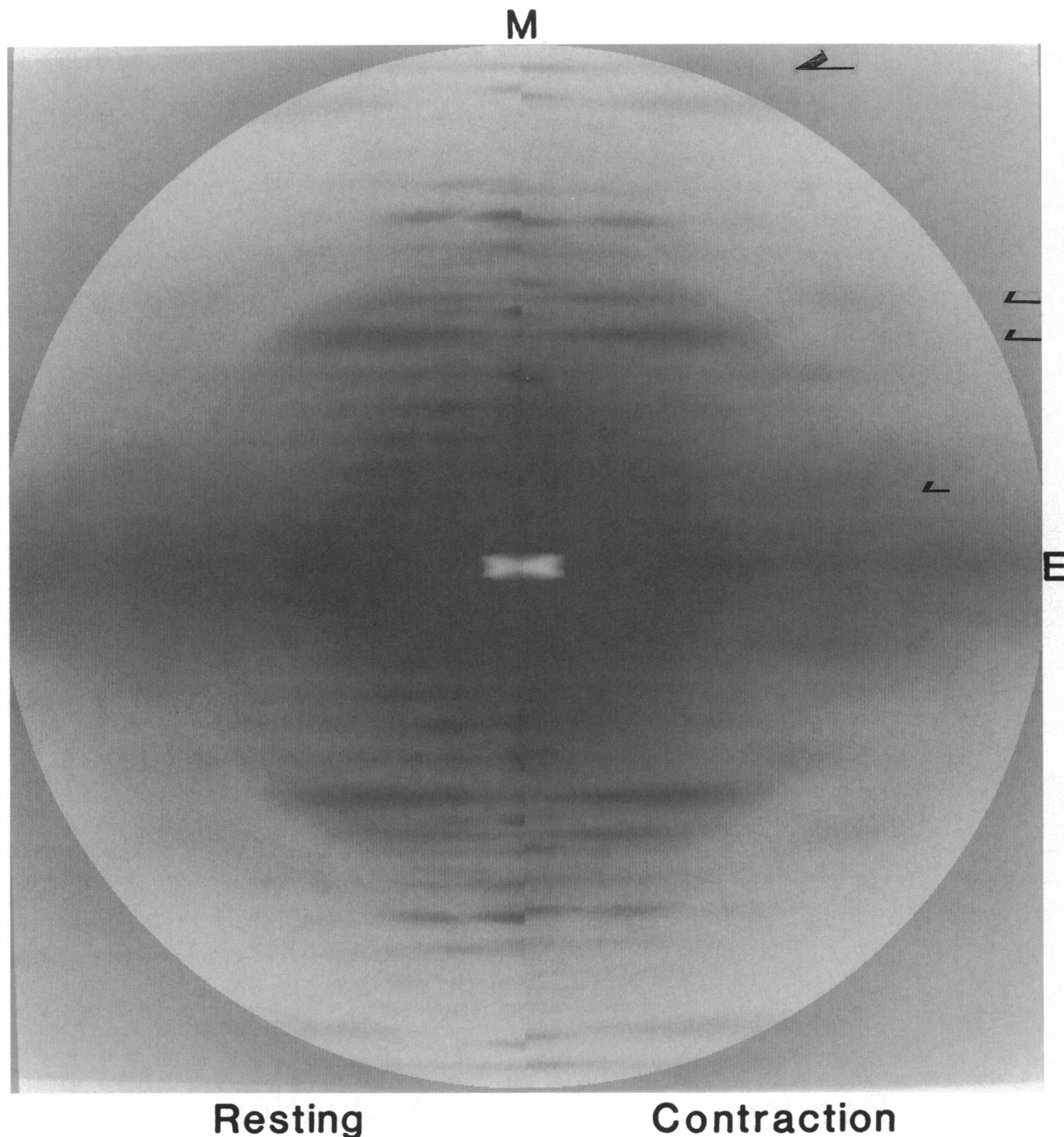
## RESULTS

Fig. 1 shows a pair of x-ray diffraction patterns from the resting and isometrically contracting/activating states of the muscles at full overlap length of the thin and thick filaments (A) and nonoverlap length (B). In Fig. 1 A, all of the myosin filament-based layer lines are markedly weakened during contraction, but the reflections indexing on integral orders of the 14.3 nm cross-bridge repeat remained strong on the meridian. The actin filament-based layer lines are intensified during contraction as reported previously (Amemiya et al., 1987; Wakabayashi and Amemiya, 1991). Myosin filament-based reflections in the contracting pattern shifted systematically toward the equator, but such a large change was not seen on any of the actin filament-based reflections. However, we found a small but distinct shift of the 2.7 nm actin meridional reflection (*arrow* at the top of Fig. 1 A) towards the equator. When muscles at nonoverlap length were stimulated, the intensities of both myosin and actin filament-based layer lines changed very little. Although it was broad, the so-called actin second layer line at  $\sim 18.5 \text{ nm}$  axial spacing became intensified at a high reciprocal radial position centered around  $R \sim 1/4 \text{ nm}^{-1}$  (see Fig. 1 B, *small arrow*), indicating that the muscle was activated by the stimuli (Kress et al., 1986; Yagi and Matsubara, 1989; Wakabayashi et al., 1991). During contraction of muscles at  $\sim$ half overlap length (not shown here), the diffraction pattern showed rather similar features to those seen in the pattern from muscles at full overlap; the loss of the myosin layer-line pattern was much greater than that expected simply from the reduced amount of filament overlap.

In general, stretching of the resting muscle weakened the myosin reflections and made most of the lattice sampling effect on the layer lines disappear (Haselgrove, 1975). When the resting patterns of Fig. 1, A and B were compared, stretching the muscle to the nonoverlap length had much more effect on the myosin meridional reflections than on the layer lines; the meridional reflections became weaker (particularly “forbidden” reflections (see Huxley and Brown, 1967)) and broader across the meridian, and there was an increase in spacing of the meridional reflections (see below). In contrast, the actin reflections were mostly not affected by stretching.

### Spacing change of the 2.7 nm actin meridional reflection

Because the 2.7 nm meridional reflection corresponds to the periodicity of axial translation of the actin subunits in the thin filament (Huxley and Brown, 1967), its spacing change provides a direct indication of the extensibility of the actin filaments. Fig. 2 shows typical examples of the axial intensity profiles of the 2.7 nm reflection after subtraction of the background: (A) a comparison between rest and isometric contraction of the muscle at full overlap length; and (B) that between rest and activation of the muscle at nonoverlap length. The thick solid and dashed curves denote the best-fit reflection profiles obtained by Gaussian deconvolution and the thin curves the least-squares fit to the data points.



**FIGURE 1** X-ray diffraction patterns of frog skeletal muscles recorded with storage phosphor plates (imaging plates). (A) A comparison of resting and isometrically contracting patterns from sartorius muscle at full overlap length of the thin and thick filaments. (B) A comparison of resting and activated patterns from semitendinosus muscle at nonoverlap length. In A and B, half of each pattern is shown with the meridional axes (vertical) aligned with each other. E, the equator; M, the meridian. The long arrow at the top indicates the 2.7 nm actin meridional reflection. The middle pair of arrows shows the 5.1 and 5.9 nm actin layer lines. A short arrow shows an intensification of the second actin layer line on activation. (Note that the intensification of the second layer line in the overstretched muscles is not as large as in the full-overlap muscles (Wakabayashi et al., 1991).)

The data points were obtained after radial integration of the intensities in the reciprocal radial range of  $0 \leq R \leq 0.053 \text{ nm}^{-1}$ . In general, the reflections were slightly asymmetric, but the present Gaussian fitting proved to be an adequate approximation for the observed data. The 2.7 nm reflection

is partially overlapped by a 16th order myosin reflection (M16) of the basic 42.9 nm repeat on the high-angle side. There is a weak 15th order myosin reflection (M15) on the low-angle side, sufficiently far away so that it did not overlap the actin reflection. During contraction, M16 fused with the

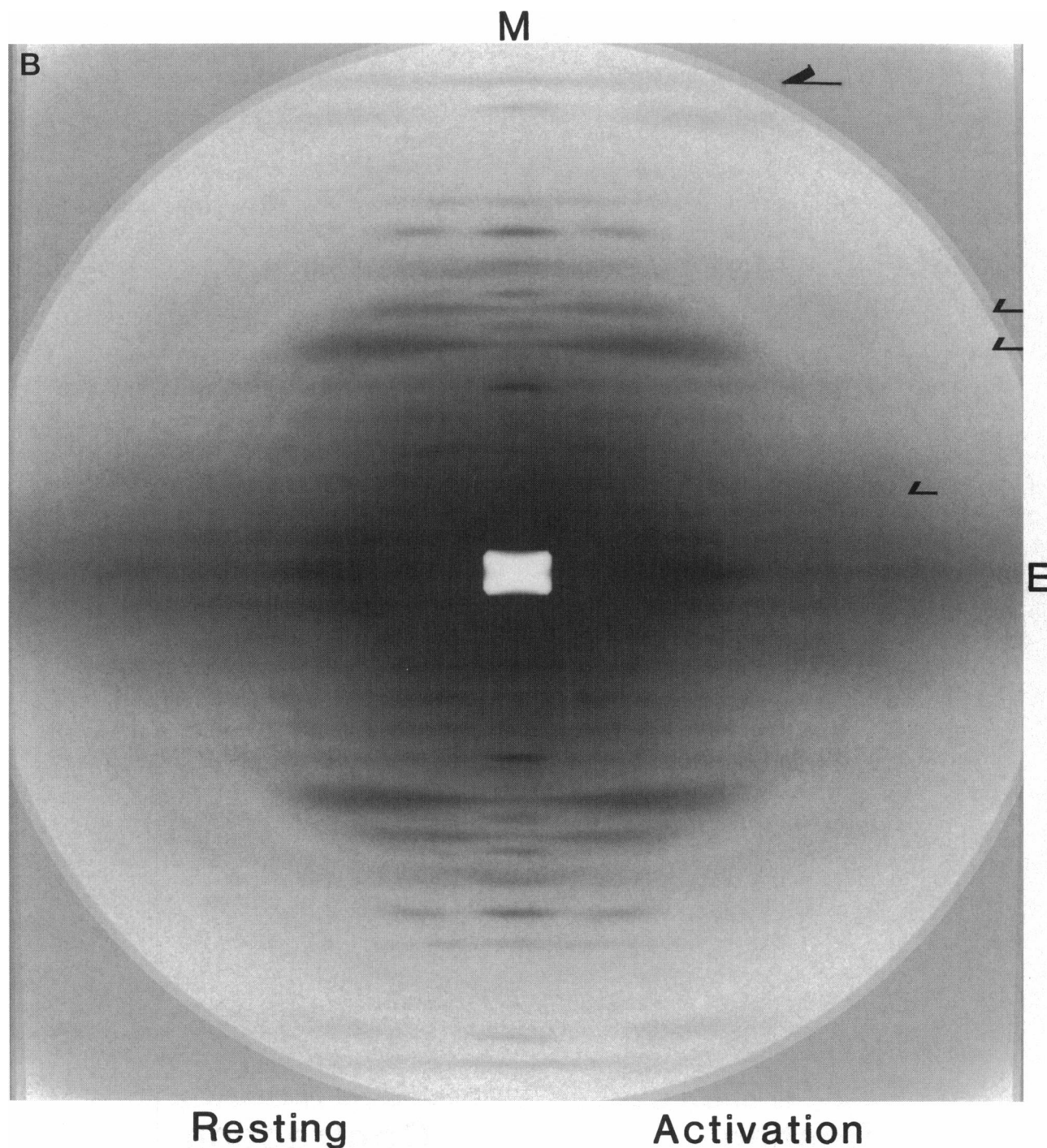
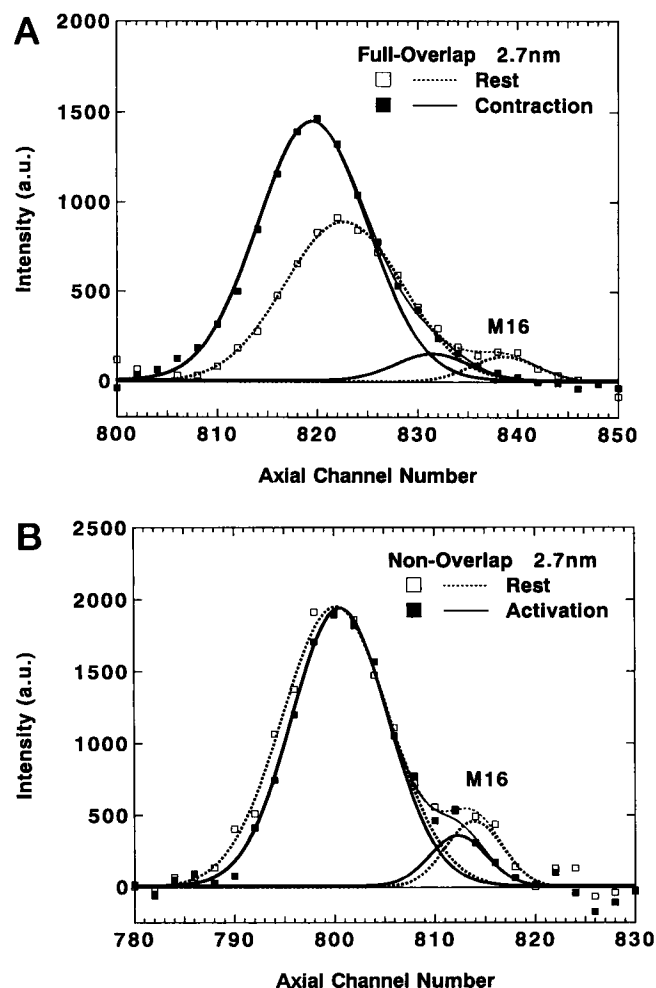


FIGURE 1 Continued

2.7 nm reflection by shifting inwards, producing a tail on the actin reflection. Although it was not clear whether the M16 reflection, which is forbidden if the myosin filament structure has a perfectly helical order, was still present during contraction, Huxley et al. (1994) in the accompanying paper observed this reflection as a more prominent shoulder in the pattern from a contracting muscle during stretch. The Gaussian separation clearly shows that during contraction of the muscles at full overlap, the intensity profile of the 2.7 nm

reflection shifted toward the low-angle side and became considerably more intense ( $\sim 1.7$ -fold) (Fig. 2 A). In this example, the 2.7 nm intensity peak moved by  $\sim 2$  pixels, corresponding to about 0.25% change in the spacing. In this reciprocal radial range, the axial intensity profile of this reflection was not appreciably altered during contraction when the peak heights of the resting and contracting profiles were normalized to each other. Measurements were also made for the muscles at half-overlap length (not shown); a similar but





**FIGURE 2** Examples of comparison of background-subtracted axial intensity profiles of the 2.7 nm actin meridional reflections at rest and during isometric activation of muscles. (A) A muscle at full overlap length; (B) A muscle stretched to nonoverlap length. Data points were obtained by radial integration of the intensities in the reciprocal radial range of  $0 \leq R \leq 0.053 \text{ nm}^{-1}$ . The abscissa is the axial pixel number spaced on a  $100 \mu\text{m}$  grid on the imaging plate. The thick curves denote the best-fit reflection profiles obtained by Gaussian deconvolution during contraction (—) and at rest (.....). The thin curves represent sum of the Gaussian components fitted by the least-squares to the data points. Larger pixel numbers indicate a larger diffraction angle. M16 denotes the sixteenth order myosin reflection of the basic  $42.9 \text{ nm}$  repeat.

smaller shift was observed for this actin reflection. Upon activation of muscles at nonoverlap length, however, the 2.7 nm reflection profile shifted slightly in the opposite direction without changing intensity (Fig. 2 B), although the M16 reflection still moved inwards. Analyses of several other sets of data gave similar results, and no significant difference was observed between sartorius and semitendinosus muscles at full- and half-overlap length.

The resulting spacing changes of the 2.7 nm actin reflection relative to their resting values for the three different values of filament overlap are summarized in Fig. 3. As shown in Fig. 3, during isometric contraction of the muscles at full overlap, the spacing of the 2.7 nm actin reflection increased on average by 0.25%. The change at ~half overlap

tended to be slightly greater than half that at full overlap. When scaled linearly up to full isometric tension, the half-overlap data gave an average increase of  $\sim 0.3\%$ . Taken together, the 2.7 nm spacing increases by 0.25–0.3% in a maximum isometric contraction. Conversely, it decreased by  $\sim 0.1\%$  upon activation of muscles stretched to nonoverlap length. If this 0.1% decrease at nonoverlap also takes place during an initial activation process at full overlap, Ca-activation may cause a slight shortening of the actin filaments immediately after the onset of stimulation, and subsequent force generation by actomyosin interaction extends the actin filaments from the shortened length. In that case, the extension of the actin filaments caused by the applied force would amount to 0.35–0.4% when the muscle switches from the relaxed to the maximum isometric tension.

### Spacing changes of the 5.1 and 5.9 nm actin layer-line reflections

The behavior of the axial spacings of the 5.1 and 5.9 nm actin layer-line reflections has also been examined. These two relatively strong reflections arise from the pitches of the right-handed and left-handed genetic helices that connect the actin subunits in the thin filaments (Huxley and Brown, 1967). Their spacing changes yield information on the mode of elongation of the actin filament. The spacing measurement was initially done in the reciprocal radial range of  $0 \leq R \leq 0.053 \text{ nm}^{-1}$ , where the layer lines show little broadening in the axial direction. Beyond this upper limit of  $R$ , they start to broaden because of arcing and their shape changes somewhat during contraction (see *pairs of thin arrows* in Fig. 1); the centroid of their axial profile shifted gradually toward the equator with increasing distance from the meridian (Wakabayashi et al., 1992). However, as mentioned in Materials and Methods, there are meridional peaks of non-helical origin at axial spacing very near both of these actin layer lines; the meridional peak at  $\sim 5.1 \text{ nm}$  is weak and diffuse, whereas that at  $\sim 5.9 \text{ nm}$  is strong and sharp. Although they might come from the same origin as the layer lines, for instance by some perturbation of the actin helix, as was suggested by experiments with orientated F-actin gels (Popp et al., 1986), when we carefully inspected some of our best oriented relaxed patterns recorded using highly collimated laboratory x-rays (after a suggestion by Prof. H. E. Huxley), we found that the axial position of the meridional peak at  $\sim 5.9 \text{ nm}$  was at a very slightly smaller reciprocal spacing than the layer line. The positional difference of the meridional peak at  $\sim 5.1 \text{ nm}$  was less discernible. The intensity behavior was different from that of the rest of layer lines; the intensities of the meridional components of both layer lines decreased during contraction or by passive stretching of the resting muscle (see the resting patterns in Fig. 1, A and B). Thus, we judged that they originate from the other diffracting structures in the sarcomere or are sampling reflections of the long range sarcomere structure, and finally settled on investigating the spacings of these two layer lines in the radial range of  $0.013 \leq R \leq 0.053 \text{ nm}^{-1}$  to

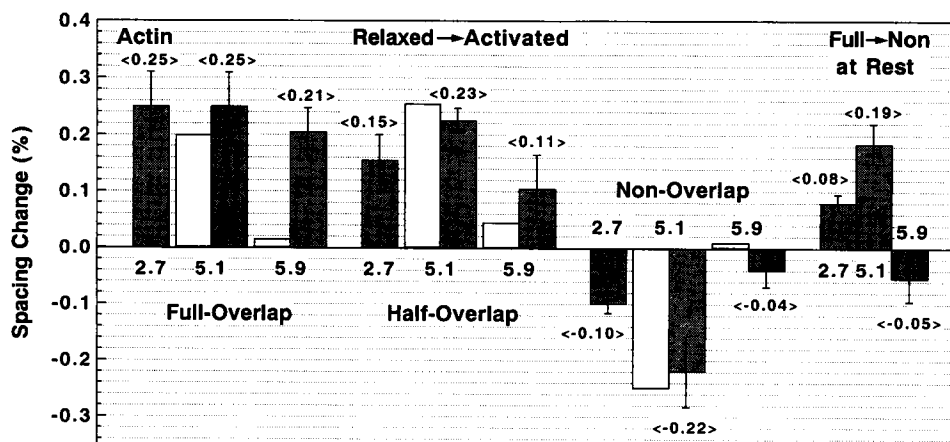


FIGURE 3 Spacing changes of the 2.7 nm actin meridional, and the 5.1 and 5.9 nm actin layer-line reflections during activation. The measurements were done in the reciprocal radial range of  $0 \leq R \leq 0.053 \text{ nm}^{-1}$  for the 2.7 nm reflection and in the range of  $0.013 \leq R \leq 0.053 \text{ nm}^{-1}$  for the 5.1 and 5.9 nm reflections. The bars indicate changes relative to the resting spacing. For reference, rest to active changes for the 5.1 and 5.9 nm reflections, measured in the radial range of  $0 \leq R \leq 0.053 \text{ nm}^{-1}$  including the meridional intensity, are also shown as white bars (see text). In the last set of bar graphs, the spacing changes of the reflections when the resting muscle was stretched from full overlap to nonoverlap length are expressed relative to the spacing at full overlap. Calculation of the bar graph was done from the four-quadrant-averaged pattern. Each set of the bar graph is the mean of three observations, each of which came from three muscles. The mean of observations is plotted along with their associated SDs. Near each bar the average value is given in braces.

exclude the meridional peaks. The range covered  $\sim 20\%$  or more of the whole layer-line intensity.

Fig. 4 shows background-subtracted axial intensity tracings of these layer lines at  $0.013 \leq R \leq 0.053 \text{ nm}^{-1}$ . The layer-line profiles in this range do not become greatly altered during contraction. Strong myosin reflections of the basic 42.9 nm repeat partially overlapped the tails of the actin reflections both on their high- and low-angle sides; the eighth (M8) and ninth (M9) order reflections approached the 5.1 nm reflection, and the seventh (M7) order and M8 reflections were near the 5.9 nm reflection, particularly M7. During isometric contraction of the muscles at full overlap, M7 disappeared and M8 became markedly broad and weak, whereas M9 intensified ( $> \text{twofold}$ ). (Note that data from the most intense part ( $0 \leq R \leq 0.013 \text{ nm}^{-1}$ ) of the myosin meridional reflections are removed in Fig. 4.) The intensity peaks of the M8 and M9 reflections shifted to lower angles. Fig. 4, A and B reveal that during contraction the intensified profiles of both the 5.1 and 5.9 nm reflections shifted toward the equator, indicating their spacing increases.

In Fig. 3 (*hatched bars*) the results of the spacing changes of these layer lines are summarized and compared with the results from the 2.7 nm reflection. During contraction of the muscles at full overlap, the average change of the 5.1 nm spacing was 0.25%, almost the same as that of the 2.7 nm reflection. Nearly the same change was also observed in the 5.1 nm spacing during contraction of the muscles at half overlap length. The 5.9 nm spacing increased by about 0.2% during contraction of the muscles at full overlap and by about 0.1% during contraction at half overlap. For reference, the initial results, including the meridional peaks, are also shown in Fig. 3 (*open bars*). The spacing change of the 5.1 nm reflection was not markedly altered by including or excluding the meridional peak. On the other hand, the spacing

change of the 5.9 nm layer line was influenced greatly by inclusion of the meridional peak; the spacing hardly changed at all on activation at full overlap (*open bar*, full-overlap, 5.9 nm in Fig. 3). This difference seemed to occur because the spacing of the meridional reflection at  $\sim 5.1 \text{ nm}$  follows the changes of the rest of the layer line, whereas that of the meridional peak at  $\sim 5.9 \text{ nm}$  moves very little during contraction. The meridional intensity at  $\sim 5.9 \text{ nm}$  at rest constitutes a considerable proportion ( $\sim 20\%$ ) relative to the inner part of the rest of the layer line. Thus, we adopt the results excluding the meridional components of these layer lines to avoid ambiguity.

Upon activation of the muscles at nonoverlap length, the 5.1 nm layer line moved in the opposite direction toward smaller spacing (Fig. 4 C). The spacing decrease was approximately double that of the 2.7 nm reflection (*hatched bar*, nonoverlap, 2.7 nm in Fig. 3). The change of the 5.9 nm spacing was very small but tended to occur in the same direction (Fig. 4 D and *hatched bar*, nonoverlap, 5.9 nm in Fig. 3). Thus, activation of overstretched muscle decreased the spacings of the actin reflections to different extents. Although the 5.9 nm intensity remained unchanged, the intensity of the 5.1 nm reflection decreased slightly in this radial range, implying a structural change of the thin filaments on activation of overstretched muscles (see Fig. 4, C and D). A consistent tendency observed in Fig. 3 (*hatched bars*) was that the spacing change of the 5.9 nm layer line was less than that of the 5.1 nm layer line on activation. Thus, the behavior of the two layer lines was also different when the thin filaments were subjected to active tension. This finding suggests that elongation of the actin filament is associated with a change in its helical structure. Based on geometrical considerations of the helical net of the actin filament (see Discussion), this change may be caused by an untwisting of the

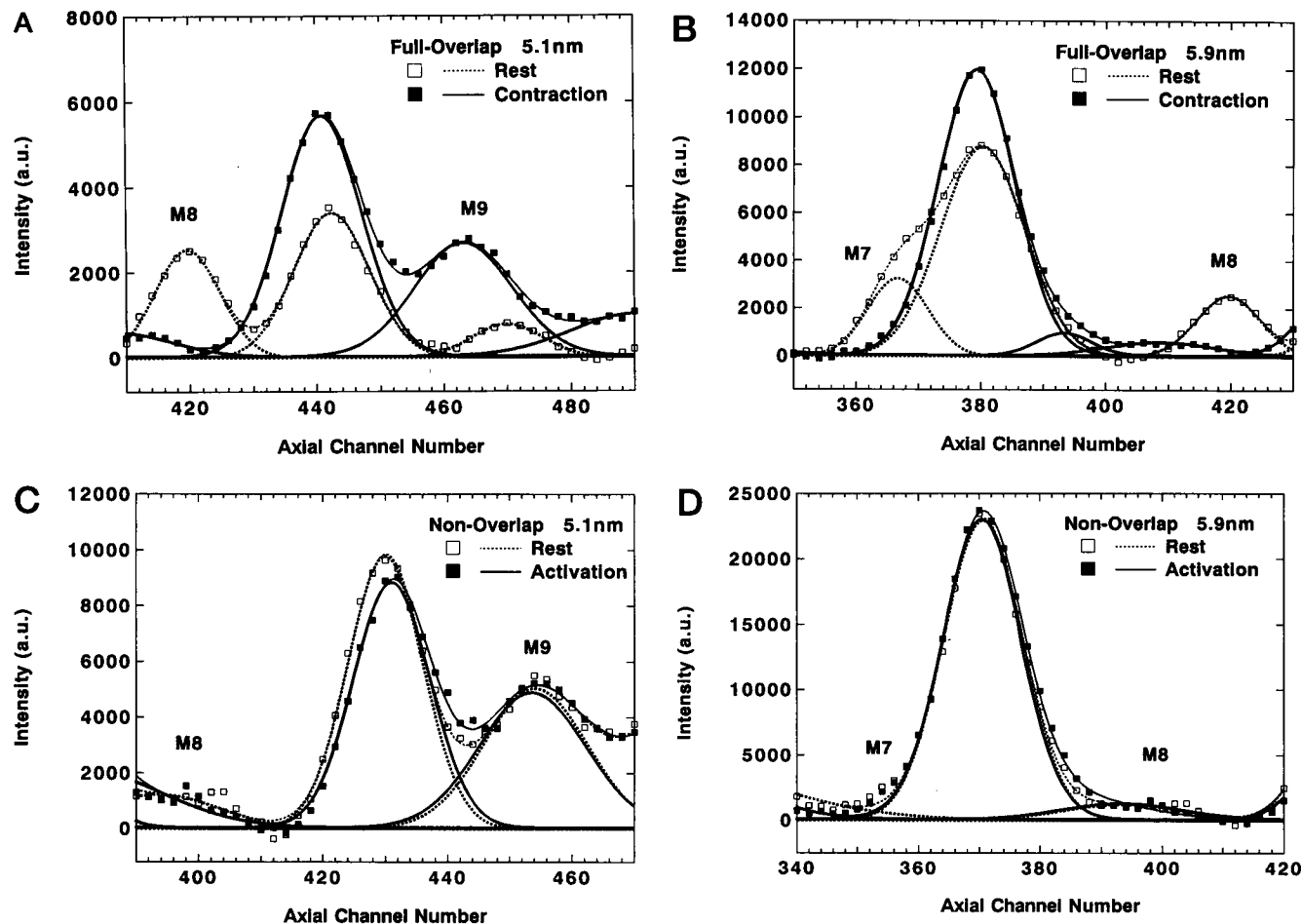


FIGURE 4 Examples of background-subtracted axial intensity profiles of the 5.1 and 5.9 nm actin layer-line reflections at rest and during activation of muscles. Data points were obtained by radial integration of intensities in the reciprocal radial range of  $0.013 \leq R \leq 0.053 \text{ nm}^{-1}$ . The 5.1 and 5.9 nm reflections are shown at full overlap length (A and B) and at nonoverlap length (C and D). M7, M8, and M9 denote the seventh, eighth, and ninth order myosin reflections of the basic 42.9 nm repeat. The symbols and curves are as shown in Fig. 2. Note that the most intense part of the intensities of the myosin meridional reflections has been removed.

right-handed genetic helix more than that of the left-handed one upon application of force. Activation itself caused a slight twisting of the right-handed helix, producing slight shortening of the actin filament in overstretched muscle.

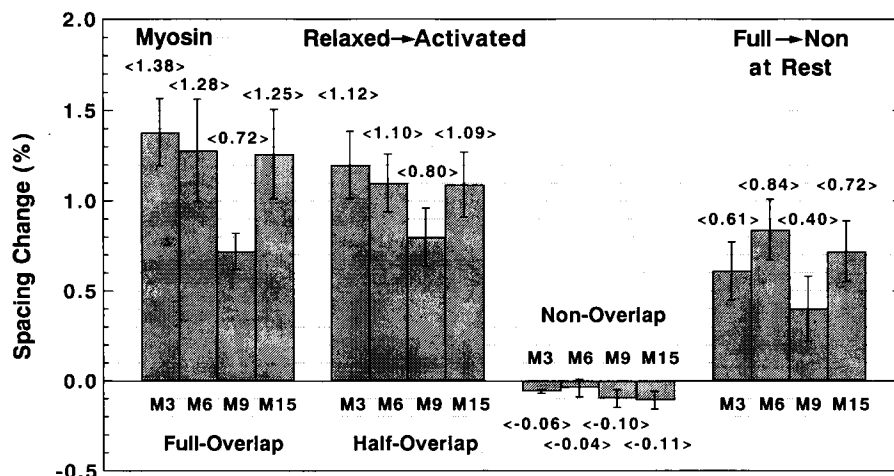
It is worth mentioning briefly the effect of stretch of the resting muscle itself on the actin spacings. The last set of bar graphs in Fig. 3 shows the spacing changes of the actin reflections when muscles were stretched from full overlap to the nonoverlap length at rest. Stretching brought about  $\sim 0.08$  and  $\sim 0.19\%$  increases in the 2.7 and 5.1 nm spacings, respectively. In contrast, the 5.9 nm spacing decreased on average by 0.05%. The changes between full- and half-overlap were much smaller than those at nonoverlap length; the spacings tended to decrease slightly but change within 0.05%. In the present experiments, passive tension seemed to be comparable with or less than the maximum tension upon activation at this overstretched muscle (see Materials and Methods). Although the spacing changes in overstretched muscles might be thought to result from the passively applied tension, the mechanism for this is uncertain.

### Spacing changes of the myosin filament-based meridional reflections

The spacing changes of the myosin filament-based meridional reflections, the third (M3), sixth (M6), ninth (M9), and fifteenth (M15) orders of the basic 42.9 nm repeat, were measured in the same manner as for the actin meridional reflection by radial integration of the intensities in the reciprocal range of  $0 \leq R \leq 0.032 \text{ nm}^{-1}$ , where most of their intensities were located. The results are summarized in Fig. 5. Our present results are in general agreement with those of the previous studies (Huxley and Brown, 1967; Haselgrove, 1975; Huxley et al., 1982; Bordas et al., 1993), indicating a large increase in the spacing of the myosin filament reflections. During isometric contraction of the muscles at full overlap, the increase in the myosin periodicity as determined by averaging the changes of each reflection was  $\sim 1.2\%$ , although the increase of the M9 reflection was smaller than that of the other reflections. During contraction of the muscles at  $\sim$ half overlap length, it was  $\sim 1\%$ . Similar to the behavior of the intensities, the change in the myosin



FIGURE 5 Spacing changes of the myosin meridional reflections during activation. M3, M6, M9, and M15 denote the third, sixth, ninth, and fifteenth order myosin reflections of the basic 42.9 nm repeat. Radial integration was made in the reciprocal range of  $0 \leq R \leq 0.032 \text{ nm}^{-1}$ . In the first three sets of bar graphs, the changes are expressed relative to the resting spacing at the same length. The last set of bar graphs shows changes when the resting muscles were stretched from full overlap to nonoverlap length. The changes are expressed relative to the spacing observed at full overlap length. The bar graphs and associated SDs are plotted as in Fig. 3.



periodicity at 3–3.2  $\mu\text{m}$  striation spacing ( $\sim$ half-maximum force) was greater than that expected from the small amount of filament overlap. In contrast, upon activation of overstretched muscles, the change in the periodicity was only  $\sim 0.08\%$  and tended to occur in the reverse direction. Thus, a change in the myosin periodicity seemed to occur that was similar to that in the actin periodicity upon activation of overstretched muscle. As shown in the last set of bar graphs in Fig. 5, stretching the resting muscle to nonoverlap length caused an increase in the myosin periodicity by  $\sim 0.6\%$  on average. This change was significantly less than that in isometric contraction of the shorter muscles, but much greater than that occurring in the actin periodicity. The change induced by stretching the resting muscle to  $\sim$ half overlap length was  $\sim 0.09\%$ . The relatively large spacing change upon overstretching the resting muscle may be related to some effect of stretching connectin/titin that links the thick filaments and the Z-line (e.g., Wang et al., 1993). However, as mentioned previously, stretching of the resting muscle caused loss of the characteristic resting order of myosin heads around the thick filament backbones and markedly decreased the intensities of the forbidden meridional reflections, accompanying the spacing increase of the myosin reflections. Most part of the apparent large spacing increase upon overstretching the resting muscle seemed to be effected by the partial removal of the systematic axial perturbation of the cross-bridge repeat (see Discussion).

### Effect of a slow stretch to a contracting muscle

When a muscle tetanized at full overlap length was stretched during tension plateau at a constant speed, the tension began to rise quickly and then increased steadily to a peak by 50–70% higher than the isometric tension level. The x-ray patterns were recorded for 0.8 s during the isometric plateau and for 0.8 s during a 1.1 s stretch, when tension was 30–70% (on average  $\sim 50\%$ ) above the isometric plateau level. Only the spacings of the 5.1, 5.9, M3, M6, and M9 reflections were measured in the same protocol as above. The spacing changes of these reflections expressed relative to their initial isometric contraction values are summarized in Fig. 6.

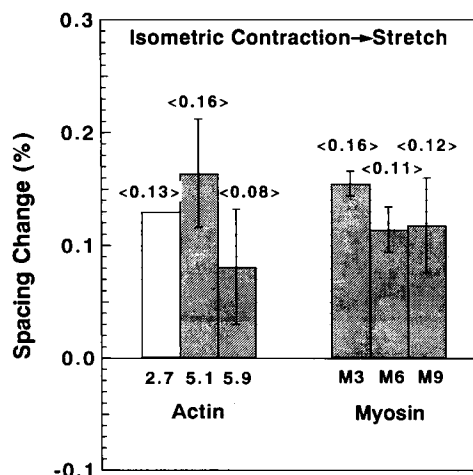


FIGURE 6 Spacing changes of the actin and myosin reflections when slow stretches were applied to isometrically contracting muscles at full overlap length. The changes are expressed relative to the initial isometric contraction spacing. Above each bar, the average value from three sets of data is shown with SDs calculated as in Fig. 3. In the first set of bar graphs, the 5.1 and 5.9 nm spacings were measured in the radial range without the meridional peaks. The change of the 2.7 nm reflection denoted by a white bar was calculated from the geometrical relation describing the actin helical net by using the average changes of the 5.1 and 5.9 nm spacings (see text). The other bars are plotted as in Figs. 3 and 5.

Stretching of a contracting muscle increased the 5.1 nm spacing by  $\sim 0.16\%$  above the isometric contraction level and simultaneously caused a smaller increase ( $\sim 0.08\%$ ) in the 5.9 nm spacing. The spacing changes seemed to occur in parallel with tension changes. Although we could not directly measure the 2.7 nm spacing during the stretch (see Materials and Methods), it could be estimated on the basis of geometrical considerations of the actin helical net using the changes of these two layer lines (see below). This estimate implies that the spacing increase of this reflection during the stretch would be  $\sim 0.13\%$  above the initial isometric contraction value (see Fig. 6), yielding a further extension of the actin filaments. When the 2.7 nm spacing change was scaled linearly up to a 100% tension increase, about 0.26% change would be predicted, agreeing well with the value

(0.25–0.3%) obtained for the isometric tension development. The intensities of the 5.1 and 5.9 nm layer lines changed only slightly during the stretch, suggesting that the number of myosin heads associated with actin remained nearly unchanged.

The M3, M6, and M9 spacings also changed during the stretch. They showed a small increase ( $\sim 0.13\%$  on average) with respect to the isometric contraction value (Fig. 6), much less pronounced than the average increase ( $\sim 1.2\%$ ) in an initial isometric contraction, suggesting extensibility of the myosin filaments. When scaled to a 100% tension increase, the change would represent an average increase of about 0.26%, in addition to the increase during isometric tension development. This change in the myosin periodicity is comparable with that seen in the actin periodicity. The intensities of the M3 and M6 reflections decreased, whereas that of the M9 reflection increased slightly during the stretch. These intensity changes indicate either a change in the axial distribution or a conformational change of the cross-bridges themselves.

## DISCUSSION

### Extensibility of the actin filaments

The present experiments revealed a distinct extensibility of the thin filaments, as evidenced by the spacing change of the 2.7 nm actin meridional reflection when live frog skeletal muscles contracted isometrically. At maximum isometric tension, the increase in the 2.7 nm spacing was found to be 0.25–0.3% relative to the value at rest. On activation of over-stretched muscles, we found that this spacing decreased by  $\sim 0.1\%$ , indicating that Ca-activation by stimulation does not cause extension but causes a slight shortening of the thin filaments. If the 0.1% decrease at nonoverlap also takes place in an initial activation process at full overlap, then the 0.3% change we observe corresponds to as much as a 0.4% increase as the overall tension-related extension in a maximal isometric contraction.

Slow stretching of a contracting muscle produced a further increase ( $\sim 0.13\%$ ) of this reflection spacing over the isometric contraction value. A value scaled up to a 100% tension increase was  $\sim 0.26\%$ , corresponding to the value for the initial isometric tension development. This result differs from the  $\sim 0.4\%$  value expected above when the muscle going from relaxation to full isometric contraction. Although this difference must be examined further, the present slow stretch result implies that up to 0.3% spacing change corresponds to the mechanical stretch of thin filaments by the maximum isometric tension. The 0.1% change we observed at nonoverlap length is probably caused by structural changes associated with the activation mechanism in the thin filaments. The extension of the actin filaments might result from the attachment of myosin heads.

The spacing measured represents the axial distance between actin monomers averaged over the whole thin filament in sarcomere. During isometric contraction, the tension distribution along each actin filament would be nonuniform; it is constant (maximal) in the I-band region and decreases linearly down to zero at the end of the overlap zone where

thin filaments terminate (White and Thorson, 1973). Such a distribution of stress along the filaments would be expected to produce nonuniformity in the actin periodicity, skewing the reflection profile. We could not observe, however, an appreciable skewing of this reflection during contraction. The effect of nonuniform spacing might be masked by the fairly large Gaussian-shaped beam width relative to the natural width of the reflection and by partial overlap with nearby reflections.

We can derive the relationship between the observed spacing change representing the average change in the actin period and the total filament extension under maximum isometric tension. The average extension of the filament per unit length designated by  $\Delta L/L$  can be expressed as

$$\Delta L/L = (\Delta L_I + \Delta L_O)/(L_I + L_O),$$

where  $L_I$  and  $L_O$  denote the length of the filament part in the I-band region and that of the filament part in the overlap zone, and  $\Delta L_I$  and  $\Delta L_O$  denote the extension of the filament part in the I-band region and that of the filament part in the overlap zone, respectively. When  $\Delta L_O/L_O$  is assumed to be half that of  $\Delta L_I/L_I$ , the above equation reveals that  $\Delta L/L = 0.675 \times (\Delta L_I/L_I)$ ; the average extension per unit length of the actin filament ( $1 \mu\text{m}$  long ( $L_I + L_O$ )) would be  $\sim 0.68$  times that of the maximal extension of the filament part in the I-band region (with a  $\sim 0.35 \mu\text{m}$  length ( $L_O$ )) at a sarcomere length of  $\sim 2.3 \mu\text{m}$ . Then the following equation describes the relation between the average change in the axial repeat,  $\Delta S/S$  ( $= \Delta h/h$ , see below) and  $\Delta L/L$  using a first power relationship between the number of diffracting units and integrated intensity of the reflection,

$$\begin{aligned} \frac{\Delta S}{S} &= \frac{(\Delta L_I/L_I) \cdot (L_I \cdot F_A^2) + (\Delta L_O/L_O) \cdot (L_O \cdot F'_A{}^2)}{L_I \cdot F_A^2 + L_O \cdot F'_A{}^2} \\ &= \frac{L_I \cdot F_A^2 + (L_O \cdot F'_A{}^2)/2}{0.675 \times (L_I \cdot F_A^2 + L_O \cdot F'_A{}^2)} \cdot \frac{\Delta L}{L} \end{aligned}$$

where  $F_A$  and  $F'_A$  are the structure amplitudes of the actin monomers in the I-band part and in the overlap zone, respectively. Provided that the actin monomers in the overlap zone and I-band region contribute equally to the reflection intensity (i.e.,  $F_A^2 = F'_A{}^2$ ), the above equation reveals that the total extension of the filament per unit length ( $\Delta L/L$ ) corresponds to the observed spacing change ( $\Delta S/S$ ). In the other extreme case, if the intensity is dominated by only those actins in the overlap zone (i.e.,  $F'_A{}^2 \gg F_A^2$ ) caused, say, by the accretion of myosin heads, the above equation illustrates that  $\Delta L/L$  could be 1.35 times larger than  $\Delta S/S$ . Thus, the observed spacing change provides a minimum estimate for the total extension of the filament; the elongation of a whole actin filament  $\sim 1 \mu\text{m}$  in length amounts to at least 3–4 nm under full isometric tension in a frog muscle. This amount of elongation of the actin filament agrees well with a value expected from the thin filament compliance estimated from recent stiffness measurements of rigor fibers (Higuchi, Yanagida, and Goldman, unpublished data) and also the stiffness of the actin-tropomyosin complex, which has been

directly measured by *in vitro* nano-manipulation (Kojima et al., 1994). Funatsu et al. (1990) suggested that the fibrous protein, nebulin, which is associated with actin filaments, had little effect on the stiffness in rigor fibers.

### Changes of the actin helix

As shown in Figs. 3 and 6, upon activation in all muscles and also during stretching of a contracting muscle the spacing changes of the three actin reflections occurred to a different degree. This tendency was observed even when the muscles were stretched at rest, although the relatively smaller change of the 5.9 nm spacing occurred in the opposite direction. In the present studies, we were forced to measure the axial spacings of the 5.1 and 5.9 nm layer lines in a narrow reciprocal radial range close to the meridian where the layer lines are sharp and well defined. The axial profile did not change significantly during activation. When the reflections were analyzed beyond the upper limit of  $R \sim 0.05 \text{ nm}^{-1}$ , the apparent spacing decreased gradually because of arcing and the axial profile became broader, making precise measurements difficult (Wakabayashi et al., 1992).

The behavior of the spacing changes can yield some information about the mode of the lengthening in terms of possible changes in the helical structure. The following relation describes the relative changes in the axial repeat and the pitches of the two genetic helices (e.g., see Squire, 1981):

$$\frac{\Delta h}{h} = \left( \frac{h}{P_{5.1}} \right) \cdot \left( \frac{\Delta P_{5.1}}{P_{5.1}} \right) + \left( \frac{h}{P_{5.9}} \right) \cdot \left( \frac{\Delta P_{5.9}}{P_{5.9}} \right)$$

where  $h$  is the axial period corresponding to the 2.7 nm meridional reflection and  $P_{5.1}$  and  $P_{5.9}$  are pitches of the right- and left-handed genetic helices, giving the 5.1 and 5.9 nm layer lines, respectively.  $\Delta$  denotes spacing changes when the state of the muscle alters. The values of  $h/P_{5.1}$  ( $\approx 0.538$ ) and  $h/P_{5.9}$  ( $\approx 0.463$ ) are derived from the axial positions of these reflections in the x-ray pattern. It is clear from the above equation that if changes in any two of the parameters are known, that of the other can be deduced. In the case where  $\Delta P_{5.9} = 0$ ,  $\Delta h/h \approx 0.538 \times (\Delta P_{5.1}/P_{5.1})$ ; the percentage change of the axial repeat is nearly equal to half that of the pitch of the right-handed genetic helix. Then, if  $\Delta P_{5.1} < 0$ ,  $\Delta h/h < 0$ . In this case, the filament shortens because of a winding of the right-handed genetic helix. This behavior seems to apply to activation of overstretched muscle (Fig. 3). If  $\Delta P_{5.1} > 0$ ,  $\Delta h/h > 0$ ; an unwinding of this helix causes extension of the filament. Thus, the change of the 5.1 nm spacing or the 5.9 nm spacing alone is insufficient to determine the extensibility of the filament.

From the data in Fig. 3, the sums of the right-hand side in the above equation are 0.232 and 0.175 (in percentage units) in isometric contraction of the muscles at full- and half-overlap length, respectively, and 0.137 upon activation of overstretched muscles. These values are consistent with the relative changes in the measured axial periodicity in each case. Because the change of the 5.1 nm pitch tended to be larger than that of the 5.9 nm pitch, there is an apparent

torsional rotation in the actin helix, dependent on the mechanical load on the muscle. On developing active tension, elongation is accompanied by untwisting of the right-handed genetic helix greater than that of the left-handed one. Full tension development alleviated much of the difference between the relative changes in the pitches of the two helices, resulting in uniform extension of the filaments. If the above equation applies to the spacing changes during stretch of a contracting muscle, the spacing changes of the 5.1 and 5.9 nm layer lines imply an increase of  $\sim 0.13\%$  in the axial period (see Fig. 6). The difference between the spacing changes of these two layer lines again indicates that the right-handed genetic helix untwists to a greater extent during the stretch. There seems to be a greater tendency of the right-handed helix to unwind than the left-handed one in the present conditions. Thus, the extension of the actin filament associated with force is connected with slight changes of its helical structure.

The overall change in the azimuthal angle of each subunit relative to its neighbors in the 5.1 nm-pitch helix is only  $0.4^\circ$  at most on going from relaxation to isometric tension or stretching, suggesting that the response could well be an elastic one. In fact, Huxley et al. (1994) in the accompanying paper showed that the spacings of the pitch reflections behave quickly in response to rapid length changes applied to contracting muscles. The small changes in the actin helical symmetry would result in at most  $\sim 0.6\%$  increase of the cross-over repeat of long-pitch helical strands, thus still occurring within the framework of a nonintegral symmetry between 13 subunits/7 turns and 28 subunits/15 turns (Huxley and Brown, 1967). There is no distinct transition to an integral 28/15 symmetry, because the azimuthal angle of each subunit would need to change about  $1^\circ$  relative to its neighbor on the genetic helix to switch from the 13/7 to the 28/15 symmetry.

### Extensibility of the myosin filaments

The average spacing increase of the thick filament-based reflections seen in isometric contraction of the muscles at full overlap was 1–1.2%. If this large spacing change reflects a change in the filament length, it is too large to be attributable to a direct effect of isometric tension on the thick filament compliance (Ford et al., 1981). The cross-bridge movement and binding to actin before development of tension that accompany disordering of a systematic perturbation of their helical repeat are probably the cause of the apparent large spacing change (Haselgrove, 1975; Yagi et al., 1981; Huxley et al., 1982; Bordas et al., 1993), although interference effects between myosin heads and the thick filament backbone and a sampling effect caused by the long range sarcomere structure might affect it. However, what fraction of this change is caused by a real increase in filament length is not yet known. To obtain this information, experiments with slow stretches applied to contracting muscles were conducted, because the changes in spacing caused by large a perturbation of the cross-bridge repeat would be minimized

during the slow stretch. In the present slow stretch experiments (and those of Huxley et al. (1994) in the accompanying paper), further small increases in the myosin spacings were observed above the isometric contraction value. When scaled linearly up to a 100% tension increase, an increase in the axial periodicity of the myosin filaments was on average 0.26%. Thus, we expect that such changes could come from extensibility of the myosin filaments. Again, the observed spacing change during stretch would yield a minimum estimate of the total extension of the myosin filament per unit length under maximum isometric tension; elongation of the filament backbone  $\sim 1.6 \mu\text{m}$  in length amounts to  $\sim 2.1 \text{ nm}$  per half sarcomere. The fact that the percentage change of the myosin filament extension is comparable with that of the actin filament indicates that the myosin filament is stiffer ( $\sim$ twofold) than the actin filament.

As with the actin reflections, if the reverse change of  $\sim 0.08\%$  in the myosin periodicity observed upon activation at nonoverlap (Fig. 5) is taken into account, the tension-related extension of the myosin filaments may be even larger than the apparent observed value. Both actin and myosin filaments may be altered at a low tension level.

There was a relatively large spacing increase ( $\sim 0.6\%$ ) when the resting muscle at full overlap length was stretched to nonoverlap length. Although this may be caused by some effect of stretching connectin/titin, as mentioned previously, the forbidden meridional reflections were markedly weakened by stretching. The strength of the forbidden reflections from the resting muscle at full overlap can be explained adequately by a model involving a systematic axial perturbation of the cross-bridge repeat (Yagi et al., 1981). This perturbation is removed when the muscle contracts or passes into rigor whether or not cross-bridges are able to interact with actin. The disappearance of the perturbation in the axial direction is accompanied by disordering of cross-bridges in the azimuthal and radial directions, simultaneously producing the spacing increase of the myosin reflections (Haselgrove, 1975). Thus, the apparent large spacing change of the myosin reflections seen upon overstretching the resting muscle seems to be caused in a large part by the partial removal of the axial perturbation, rather than by an elastic backbone extension caused by the stress applied from stretching connectin/titin. To examine the effect of connectin/titin, it would be necessary to investigate in detail the spacing behavior in the resting muscle at different degrees of filament overlap and at different times during the decay of passive tension that follows the initial overstretch.

### Implications for instantaneous sarcomere elasticity

One of the conclusions of mechanical transient experiments on contracting muscle fibers was that there is instantaneous elasticity somewhere in the cross-bridge-actin assembly (Huxley, 1974). In isometric contraction, this elasticity carries tension that can be reduced to zero by a 4–6 nm per half-sarcomere shortening of the muscle (Huxley, 1974; Ford

et al., 1977, 1981). In steady-state measurements of extension associated with force, our main findings were that the thin actin and thick myosin filaments are both extensible under isometric tension. If the reverse changes in spacing observed upon activation at nonoverlap length were not taken into account, the average spacing increases of the actin and myosin meridional reflections in a maximum tension were  $\sim 0.3$  and  $\sim 0.26\%$ , respectively, each corresponding to elongation of  $\sim 3 \text{ nm}$  for the actin filaments and  $\sim 2.1 \text{ nm}$  for the myosin filaments per half-sarcomere. However, the true proportion of the spacing increase seen in isometric contraction caused by tension on the actin and myosin filaments is uncertain. The mechanical situation in steady-state and at reduced overlap (where all cross-bridges possibly exert positive tension) would be different from the dynamic situation when a quick length step is applied to contracting muscles (where zero tension should be a balance between positive and negative forces from strained cross-bridges). To distinguish directly the elastic component related to tension, one would need experiments with quick length changes applied to contracting muscles, reducing tension down toward zero. Unfortunately, we could not perform such experiments because the intensity is insufficient at the present beam line at the Photon Factory. Such experiments were tried by Huxley et al. (1994) and reported in the accompanying paper. They used a very intense beam from the multi-pole wiggler line at CHESS, USA (Irving and Huxley, 1994). As described there, Huxley et al. (1994) found corresponding changes of about 0.24% (as derived from the 5.1 and 5.9 nm spacing changes) in actin periodicity and  $\sim 0.1\%$  in myosin periodicity during 2 ms after a quick release down to almost zero tension. The change in the actin periodicity was comparable with the change predicted from our slow stretch experiments. The change in the myosin periodicity was roughly half that observed during a stretch. Although their results suggest a difference in the spacing behavior between steady lengthening and quick release, it may be insufficient to provide a decisive conclusion because some tension recovery probably occurred by the time of their x-ray measurements after quick release. Their results indicate that most of the spacing changes of the actin reflections, possibly the myosin reflections too, responded quickly to rapid length changes, suggesting that the extensibility of the actin and myosin filaments is elastic. Kojima et al. (1994) have also shown in vitro that the extensibility of the actin filament containing tropomyosin is purely elastic.

White and Thorson (1973) and later Ford et al. (1981) presented a formula that includes contributions of thin and thick filament compliance to the total instantaneous elasticity of a sarcomere. We can derive the possible contribution of the myofilament compliance to the total sarcomere compliance using the formula (A10) of Ford et al. (1981) by making a comparison of our steady data with the extrapolated intercept of the  $T_1$  curve in mechanical studies. From our x-ray data ( $\sim 0.3\%$  extension for the actin filament and  $\sim 0.26\%$  for the myosin filament under maximum isometric tension), stiffness values of the thin

and thick filaments were estimated. Because our measurements were done at 8–10°C, an extrapolated value ( $\sim 6$  nm) of the  $T_1$  curve obtained at  $\sim 8^\circ\text{C}$  (Ford et al., 1977) was used. Assuming the sarcomere structure of a frog muscle at  $\sim 2.3$   $\mu\text{m}$  length, with actin filaments 1.0  $\mu\text{m}$  long and myosin filaments 1.6  $\mu\text{m}$  long, giving I-band of  $\sim 0.35$   $\mu\text{m}$  and H-zone of  $\sim 0.15$   $\mu\text{m}$  per half-sarcomere, the contributions of the actin and myosin filaments to the instantaneous shortening ( $\sim 6$  nm) could be  $\sim 2.5$  and  $\sim 1.6$  nm, respectively, each corresponding to  $\sim 83$  and  $\sim 76\%$  of their steady extension. Thus, our x-ray results reveal that at least a 42% of the total instantaneous sarcomere compliance is caused by the actin filament extensibility, with an additional contribution of 27% from the myosin filament. We conclude that  $\sim 70\%$  of the total compliance of the activated muscle is associated with the actin and myosin filaments, in contrast to mechanical studies that have suggested that most of the compliance resides in the cross-bridges.

We wish to express our sincere gratitude to Professor H. E. Huxley for his stimulating discussions, valuable comments and long term encouragement to attain results consistent between the two groups. We are also grateful to Professor H. E. Huxley for sharing their findings before submission that were extremely useful for reanalysis of our data. Special thanks are also due to Dr. Y. E. Goldman for critical reading of the manuscript and valuable comments. We thank Professor F. Oosawa for his continuous suggestions and encouragement, Dr. T. Yanagida for showing us extensibility results on the actin filaments in vitro, Drs. K. Namba, N. Yagi, T. C. Irving and H. Higuchi for helpful discussions and comments. Finally, we would like to thank Drs. T. Kobayashi, H. Iwamoto, T. Hamanaka, Messrs. H. Saito and Y. Moriwaki for their kind help throughout the experiments at the Photon Factory. We are indebted to the Protein Institute of Osaka University for use of the NEC ACOS S-3700 computer facilities. This work was supported in part by grants-in-Aid from the Ministry of Education, Science and Culture of Japan (K. Wakabayashi).

## REFERENCES

- Amemiya, Y., S. Kishimoto, T. Matsushita, Y. Satow, and M. Ando. 1989. Imaging plate for time-resolved x-ray measurements. *Rev. Sci. Instrum.* 60:1552–1556.
- Amemiya, Y., Y. Satow, T. Matsushita, J. Chikawa, K. Wakabayashi, and J. Miyahara. 1988. A storage phosphor detector (imaging plate) and its application to diffraction studies using synchrotron radiation. *Top. Curr. Chem.* 147:120–144.
- Amemiya, Y., and K. Wakabayashi. 1991. Imaging plate and its application to x-ray diffraction of muscle. *Adv. Biophys.* 27:115–128.
- Amemiya, Y., K. Wakabayashi, T. Hamanaka, T. Wakabayashi, H. Hashizume, and T. Matsushita. 1983. Design of a small-angle x-ray diffractometer using synchrotron radiation at the Photon Factory. *Nucl. Instrum. Methods.* 208:471–477.
- Amemiya, Y., K. Wakabayashi, H. Tanaka, Y. Ueno, and J. Miyahara. 1987. Laser-stimulated luminescence used to measure x-ray diffraction of a contracting striated muscle. *Science.* 237:164–168.
- Bagni, M. A., G. Cecchi, F. Colomo, and C. Poggesi. 1990. Tension and stiffness of frog muscle fibres at full filament overlap. *J. Muscle Res. Cell Motil.* 11:371–377.
- Bordas, J., G. P. Diakun, F. G. Diaz, J. E. Harries, R. A. Lewis, J. Lowy, G. R. Mant, M. L. Martin-Fernandez, and E. Towns-Andrews. 1993. Two-dimensional time-resolved x-ray diffraction studies of live isometrically contracting frog skeletal muscle. *J. Muscle Res. Cell Motil.* 14: 311–324.
- Faruqi, A. R. 1986. Multiwire detector and data acquisition system for time resolved experiments. *J. Physiol. (Paris).* 47 C5:149–156.
- Ford, L. E., A. F. Huxley, and R. M. Simmons. 1977. Tension responses to sudden length change in stimulated frog muscle fibers near slack length. *J. Physiol.* 269:441–515.
- Ford, L. E., A. F. Huxley, and R. M. Simmons. 1981. The relation between stiffness and filament overlap in stimulated frog muscle fibres. *J. Physiol.* 311:219–249.
- Funatsu, T., H. Higuchi, and S. Ishiwata. 1990. Elastic filaments in skeletal muscle revealed by selective removal of thin filaments with plasma gel-solin. *J. Cell Biol.* 110:53–62.
- Haselgrove, J. C. 1975. X-ray evidence for conformational changes in the myosin filaments of vertebrate striated muscle. *J. Mol. Biol.* 92:113–143.
- Holmes, K. C., and J. Barrington-Leigh. 1974. The effect of disorientation on the intensity distribution of non-crystalline fibers. I. *Theory. Acta Cryst.* A30:635–638.
- Huxley, A. F., and R. M. Simmons. 1973. Mechanical transients and the origin of muscular force. *Cold Spring Harbor Symp. Quant. Biol.* 37: 669–680.
- Huxley, A. F. 1974. Muscular contraction. *J. Physiol.* 243:1–43.
- Huxley, H. E. 1973. Structural changes in the actin- and myosin containing filaments during contraction. *Cold Spring Harbor Symp. Quant. Biol.* 37:361–376.
- Huxley, H. E., and W. Brown. 1967. The low-angle x-ray diagram of vertebrate striated muscle and its behaviour during contraction and rigor. *J. Mol. Biol.* 30:383–434.
- Huxley, H. E., A. R. Faruqi, M. Kress, J. Bordas, and M. H. J. Koch. 1982. Time-resolved x-ray diffraction studies of the myosin layer-line reflections during muscle contraction. *J. Mol. Biol.* 158:637–684.
- Huxley, H. E., M. Kress, A. R. Faruqi, and R. M. Simmons. 1988. X-ray diffraction studies on muscle during rapid shortening and their implications concerning crossbridge behaviour. *Adv. Exp. Med. Biol.* 226: 347–352.
- Huxley, H. E., A. Stewart, H. Sosa, and T. C. Irving. 1994. X-ray diffraction measurements of the extensibility of actin and myosin filaments in contracting muscle. *Biophys. J.* In press.
- Irving, T. C., and H. E. Huxley. 1994. Muscle diffraction at the Cornell high energy synchrotron source. In *Synchrotron Radiation in the Biosciences*. Vol. 1, part 6. H. E. Huxley, S. Ebashi, editors. Oxford University Press, New York. 519–529.
- Julian, F. J., and D. L. Morgan. 1981. Tension, stiffness, unloaded shortening speed and potentiation of frog muscle fibres at sarcomere length below optimum. *J. Physiol.* 319:205–217.
- Kojima, H., A. Ishijima, and T. Yanagida. 1994. Direct measurement of stiffness of single actin filaments with and without tropomyosin using nano-manipulation. *Proc. Natl. Acad. Sci. USA.* In press.
- Kress, M., H. E. Huxley, A. R. Faruqi, and J. Hendrix. 1986. Structural changes during activation of frog muscle studied by time-resolved x-ray diffraction. *J. Mol. Biol.* 188:325–342.
- Makowski, L. 1978. Processing of x-ray diffraction data from partially oriented specimens. *J. Appl. Cryst.* 11:273–283.
- Oosawa, F. 1977. Actin-actin bond strength and the conformational change of F-actin. *Biorheology.* 14:11–19.
- Popp, D., W. Jahn, and K. C. Holmes. 1986. X-ray diffraction studies on orientated F-actin. EMBO-MDA Workshop Alpbach Meeting. Abstract.
- Press, W. H., B. P. Flannery, W. T. Teukolsky, and W. T. Vetterling. 1990. Numerical Recipes: The Art of Scientific Computing. Cambridge University Press, Cambridge.
- Squire, J. 1981. The Structural Basis of Muscular Contraction. Plenum Press, New York.
- Suzuki, S., and H. Sugi. 1983. Extensibility of the myofilaments in vertebrate skeletal muscle as revealed by stretching rigor muscle fibers. *J. Gen. Physiol.* 81:531–546.
- Wakabayashi, K., and Y. Amemiya. 1991. Progress in x-ray synchrotron diffraction studies of muscle contraction. In *Handbook on Synchrotron Radiation*. Vol. 4. S. Ebashi, M. Koch, and E. Rubenstein, editors. North-Holland, Amsterdam. 597–678.
- Wakabayashi, K., H. Saito, T. Kobayashi, Y. Ueno, and H. Tanaka. 1992. Detection of the spacing changes of muscle thin filaments during force generation by x-ray diffraction. *Photon Factory Act. Rep.* 10:352.
- Wakabayashi, K., H. Saito, Y. Ueno, T. Kobayashi, and H. Tanaka. 1993. Spacing changes of the thin filaments from live frog skeletal muscle

- during an isometric contraction. *J. Muscle Res. Cell Motil.* 14:360a. (Abstr.)
- Wakabayashi, K., H. Tanaka, H. Saito, N. Moriwaki, Y. Ueno, and Y. Amemiya. 1991. Dynamic x-ray diffraction of skeletal muscle contraction: structural change of actin filaments. *Adv. Biophys.* 27: 3–13.
- Wang, K., R. McCarter, J. Wright, J. Beverly, and R. Ramirez-Mitchel. 1993. Viscoelasticity of the sarcomere matrix of skeletal muscles: the titin-myosin composite filament is a dual-stage molecular spring. *Biophys. J.* 64:1161–1177.
- White, D. C. S. and J. Thorson. 1973. The kinetics of muscle contraction. *Prog. Biophys. Mol. Biol.* 27:173–255.
- Yagi, N. 1992. Effects of N-ethylmaleimide on the structure of skinned frog skeletal muscles. *J. Muscle Res. Cell Motil.* 13:457–463.
- Yagi, N., and I. Matsubara. 1989. Structural changes in the thin filament during activation studied by x-ray diffraction by highly stretched skeletal muscle. *J. Mol. Biol.* 208:359–363.
- Yagi, N., E. J. O'Brien, and I. Matsubara. 1981. Changes of thick filament structure during contraction of frog striated muscle. *Biophys. J.* 33:121–138.
- Yagi, N., S. Takemori, and M. Watanabe. 1993. An x-ray diffraction study of frog skeletal muscle during shortening near the maximum velocity. *J. Mol. Biol.* 231:668–677.